# NACA

# RESEARCH MEMORANDUM

INTERPRETATION OF BOUNDARY-LAYER PRESSURE-RAKE DATA

IN FLOW WITH A DETACHED SHOCK

By Roger W. Luidens and Robert T. Madden

Lewis Flight Propulsion Laboratory
Cleveland, Ohio

# NATIONAL ADVISORY COMMITTEE
# FOR AERONAUTICS

## WASHINGTON
December 22, 1950

# NATIONAL ADVISORY COMMITTEE FOR AERONAUTICS

## INTERPRETATION OF BOUNDARY-LAYER PRESSURE-RAKE DATA

## IN FLOW WITH A DETACHED SHOCK

By Roger W. Luidens and Robert T. Madden

## SUMMARY

A procedure is presented for determining boundary-layer quantities from pressure-rake data, which include the combined effects of viscous and shock losses. The problem is analyzed using schlieren photographs of the shock configuration, the continuity of mass relationship, and the characteristic of the turbulent boundary layer that its outer edge is defined by a rapid change in slope in the Mach number profiles in the vicinity of the edge.

## INTRODUCTION

In the general problem of studying flow about a body in a supersonic stream, the determination of the force contributed by friction and the characteristics of the boundary layer are of interest. The conventional method of determining the friction force by evaluating the momentum decrement obtained from rake measurements must be modified when strong shock waves occur in the flow ahead of the rake, because the losses in total pressure across the shock are included in the rake readings. The momentum decrement due to shock losses must therefore be separated from that associated with viscosity before the boundary-layer characteristics can be determined. Such a condition exists in the case of a ram-jet engine operating with the normal shock ahead of the inlet.

This report presents data obtained from rake measurements influenced by several different shock configurations and demonstrates a procedure that may be used to determine the boundary-layer characteristics, particularly the extent and the magnitude of the momentum decrement due to friction.

## SYMBOLS

The following symbols are used in this report:

$C_f$    skin-friction coefficient based on wetted area

P          total pressure

M          Mach number

$m_3$        measured internal mass flow

$m_0$        calculated mass flow in a free-stream tube of diameter equal
           to lip diameter

p          static pressure

$R_l$         Reynolds number based on distance from cowl leading edge to
           rake

r          radius measured from model center line

$r_{a,0}$       radius of limiting entering streamline

U          velocity at outer edge of boundary layer

u          velocity within boundary layer

y          distance from friction surface

$\gamma$          ratio of specific heat at constant pressure to specific heat
           at constant volume

$\delta$          boundary-layer thickness

$\rho$          mass density

$\varphi$          angle between shock wave and normal to free-stream

Subscripts:

a,b,c,d,   streamlines

0          free-stream conditions

1          conditions just behind bow-shock wave

2          conditions at boundary-layer rake

## METHODS AND DISCUSSION

Typical boundary-layer rake data influenced by detached shocks of
varying strength were obtained from an investigation in the Lewis 8- by

6-foot tunnel of the nose-inlet model shown in figure 1. The data were obtained at a free-stream Mach number of 1.99, a Reynolds number of 18,600,000, based on the distance from the cowl leading edge to the rake (51 in.) and at an angle of attack of 0°. The bow-shock configurations for several engine mass-flow ratios are shown in figure 2. Corresponding rake total-pressure data are presented in figure 3 as the variation of local Mach number with distance from the surface. The local Mach numbers were calculated using the Rayleigh equation with the measured total pressures and the surface static pressure ahead of the rake.

Large changes in the measured Mach number profiles with changes in mass-flow ratio or shock-wave configuration are shown in figure 3. In order to correlate the changes in Mach number distribution with shock-wave configuration, the following procedure was used to determine the theoretical shock losses for representative streamlines corresponding to several of the rake tubes. Using the notation of figure 4, the radius $r_{a,0}$, which corresponds to the entering streamline, was determined from the internal mass-flow ratio. Then by applying the continuity relation

$$ p_0 M_0 \left( 1 + \frac{\gamma-1}{2} M_0^2 \right)^{\frac{1}{2}} \left[ r_{b,0}^2 - r_{a,0}^2 \right] = 2 \int_{r_{a,2}}^{r_{b,2}} p M \left( 1 + \frac{\gamma-1}{2} M^2 \right)^{\frac{1}{2}} r \, dr $$

between streamlines at the rake and free-stream conditions, various radii such as $r_{b,0}$ were determined on the shock. From the known free-stream Mach number and total pressure and measurements on schlieren photographs (fig. 2) of the shock-wave inclination at the previously calculated radii, the total pressure behind the shock was obtained for several streamlines.

These calculated values of total pressure $(P_1)$ and the measured static pressure at the rake were used to determine the local Mach numbers, which are associated only with the losses across the shock wave. The Mach-number distribution obtained in this manner differs from that which would be calculated for no boundary-layer flow in that the Mach number at a given height of the rake has been determined for the experimental mass-flow distribution rather than for the mass-flow distribution that would exist in a frictionless flow. A comparison of the calculated and measured local Mach number distribution is presented in figure 5 for the four inlet-shock configurations shown in figure 2. The radii for which the values were determined are indicated for a mass-flow ratio of 0.376.

For the region outward from $y = 0.65$, the slopes of the curves obtained from the schlieren analysis agree well with the rake measured values. The difference in values obtained by the two methods at a given distance from the surface is greater than would be anticipated considering possible errors in measurements on the schlieren photographs.

In all cases the calculated Mach numbers are less than those determined with the rake, an unexpected result because only the bow-shock loss was considered; that is, additional unconsidered total-pressure losses would result in even lower calculated values of Mach number. The cause for the observed discrepency is unknown; however, the foregoing method neglects the possibility of turbulent mixing or momentum interchange. The Mach-number distributions due to shock losses can also be determined from the total pressure calculated using the schlieren photograph and that measured by the rake. Such a calculation, however, resulted in an improbable variation of static pressure within the rake region and no data are presented.

Because the calculated shock-loss curves of figure 5 indicate continuous and relatively uniform Mach-number variations, the rapid change in slope of the measured Mach number profiles was considered to be an indication of the extent of the boundary layer. In order to check this hypothesis, the point of most rapidly changing slope in the measured profiles was established by continuing the fairing of the upper relatively straight section $(y \sim .6$ to $1.5)$ and the lower curved section to their point of intersection. Using the thickness and Mach number at this point and assuming constant total temperature through the boundary layer, dimensionless plots were made of the profiles obtained from the data forming the lower section of the curves. The agreement of these results, which are presented in figure 6, with the 1/7 power distribution associated with turbulent flow lends support to the previously determined extent of the boundary layer.

Before the friction-momentum decrement of the boundary layer can be discussed, the shock losses within this region must be considered. Because of the relatively small increment of length on the shock wave (indicated by $r_{a,0}$ and $r_{b,0}$, fig. 2(a)) that corresponds to the mass flow in the friction layer, a negligible change occurred in Mach number due to shock losses within the boundary layer as shown in figure 5. Thus the friction for these data can apparently be determined by intergrating the momentum decrement represented by the typical shaded area of figure 5(b), where the shock-loss curve has been displaced to pass through the point corresponding to the outer edge of the boundary layer, which was previously determined from the rake data.

Skin-friction coefficients determined by means of the foregoing analysis are presented in figure 7. The calculated values are

essentially independent of mass-flow ratio and agree closely with that predicted by von Kármán's equation for compressible turbulent flow.

The preceding calculation has assumed that the rake data are correct and that the discrepancy observed in figure 5 results from a shortcoming in the procedure for calculating the total head at the rake using a schlieren photograph. If the assumption were made that calculations using the schlieren photographs are correct and the rake data are shifted to correct the edge velocity but maintain the boundary-layer thickness and nondimensional profile, the friction coefficient thus determined would be between 1 and 5 percent less than presented in figure 7.

## SUMMARY OF RESULTS

A procedure has been presented for determining boundary-layer quantities from pressure-rake data,which includes the combined effects of viscous and shock losses. The method used schlieren photographs of the shock configuration, the continuity of mass relationship, and the characteristic of the turbulent boundary layer that its outer edge is defined by a rapid change in the slope of the Mach number profiles in the vicinity of the edge. Values of friction coefficient obtained were in close agreement with those predicted theoretically for compressible turbulent flow on a flat plate.

Lewis Flight Propulsion Laboratory,
    National Advisory Committee for Aeronautics,
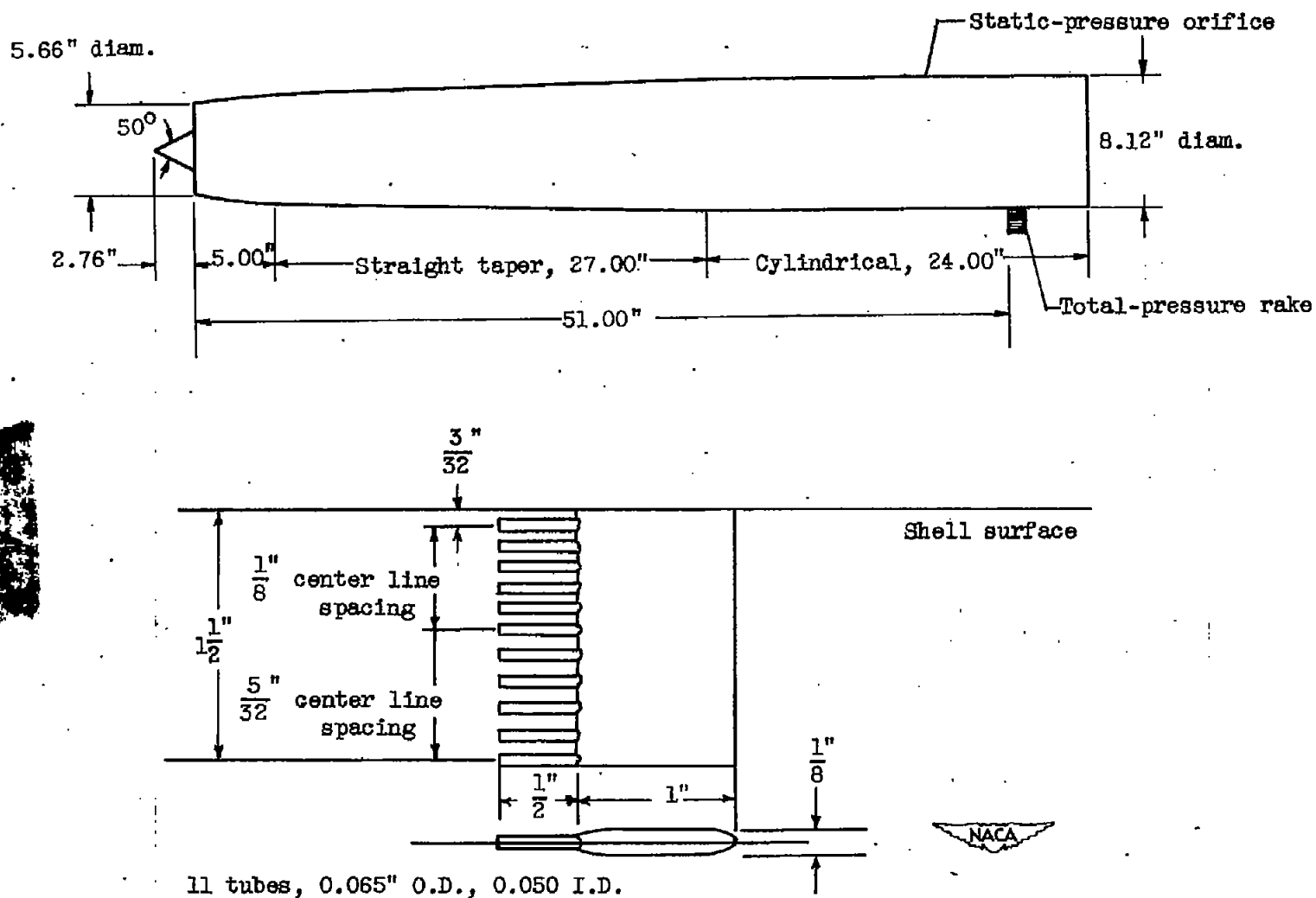        Cleveland, Ohio.

Figure 1. - Principal dimensions of model used in investigation. Maximum cross-sectional area, 0.360 square foot; wetted area ahead of rake, 8.465 square feet.
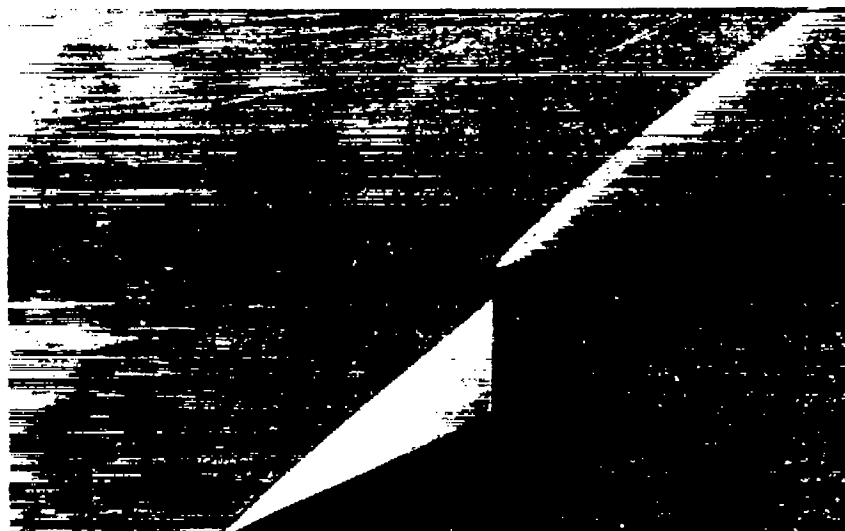
(a) Mass-flow ratio $m_3/m_0$, 0.376.



(b) Mass-flow ratio $m_3/m_0$, 0.773.

Figure 2. - Schlieren photographs of bow-shock configurations.

C-26521

(c) Mass-flow ratio $m_3/m_0$, 0.885.



(d) Mass-flow ratio $m_3/m_0$, 1.000.

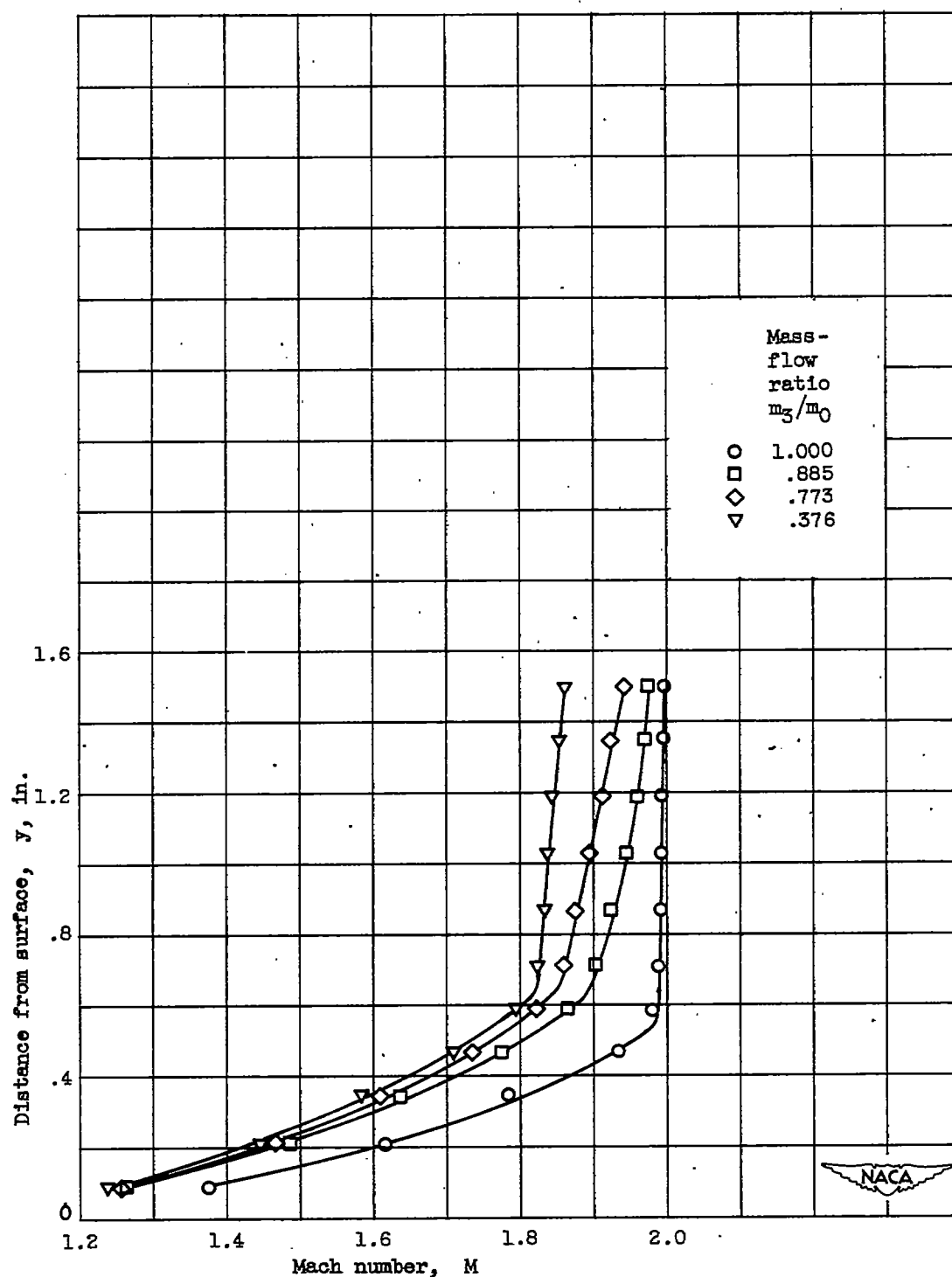Figure 2. - Concluded.  Schlieren photographs of bow-shock configurations.

C-26522

Figure 3. - Variation in measured Mach number with changes in mass-flow ratio (shock-wave configuration). Reynolds number $R_l$, 18,600,000; free-stream Mach number $M_0$, 1.99.
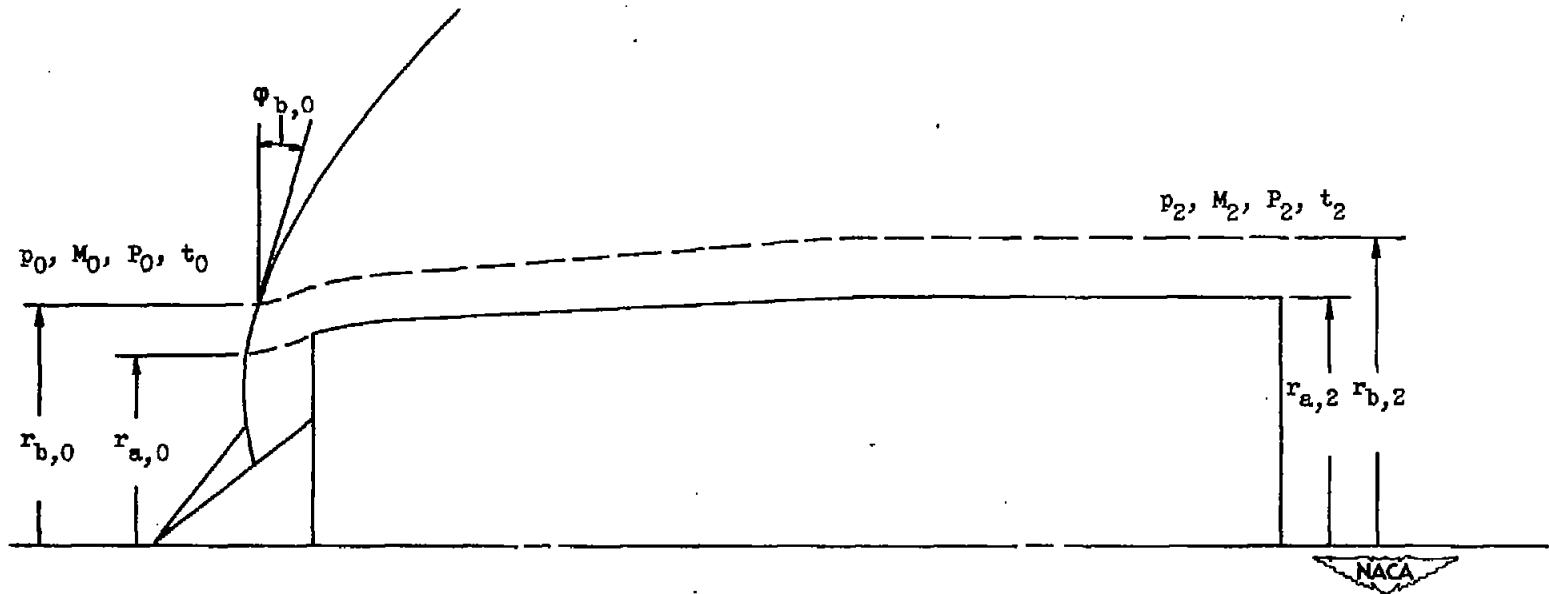
Figure 4. - Sketch showing notation used in shock-wave analysis.

(a) Mass-flow ratio $m_3/m_0$, 0.376.

(b) Mass-flow ratio $m_3/m_0$, 0.773.

(c) Mass-flow ratio $m_3/m_0$, 0.885.
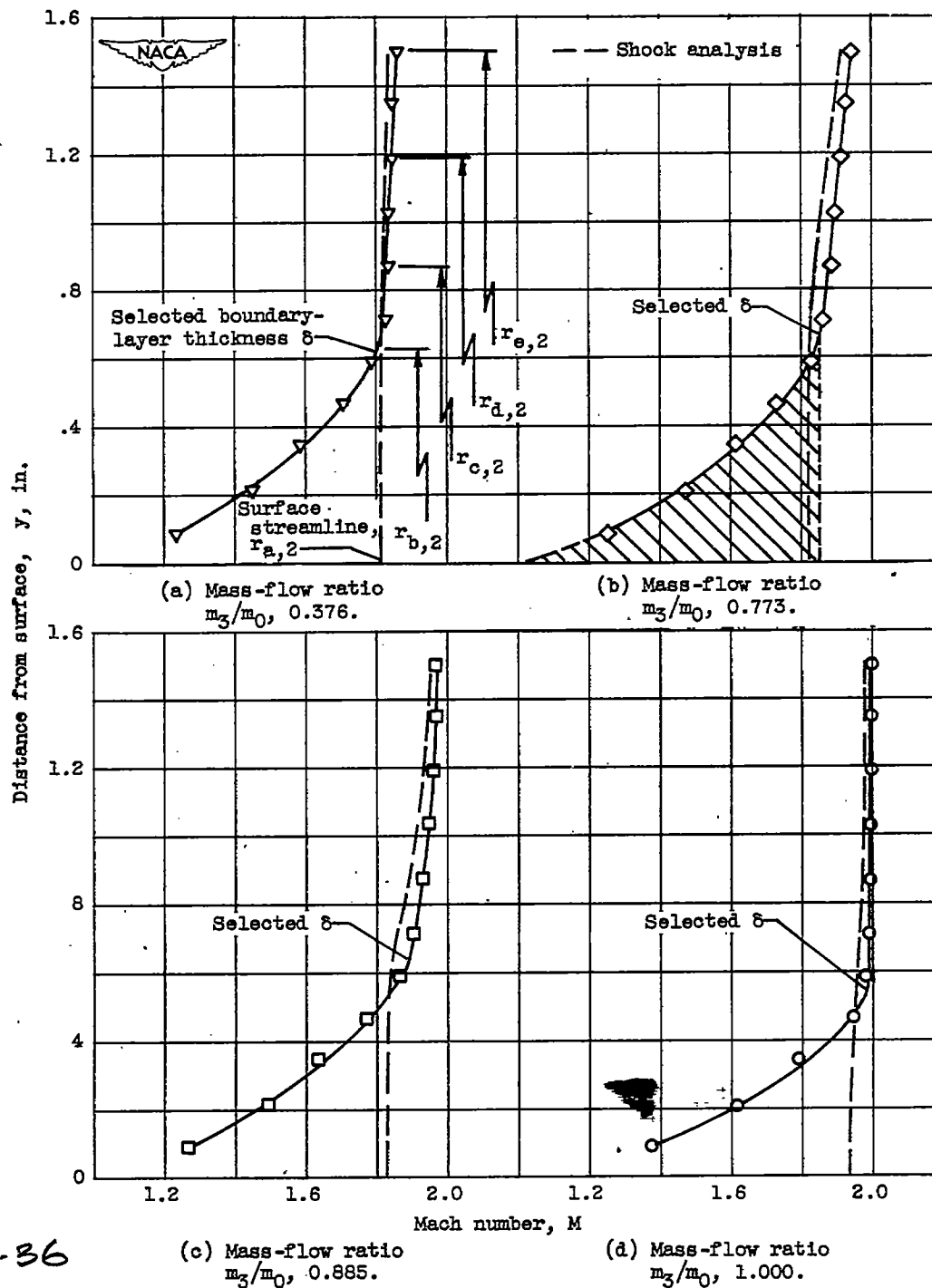
(d) Mass-flow ratio $m_3/m_0$, 1.000.

Figure 5. - Mach number profiles obtained from rake measurements and from shock-wave analysis. Reynolds number $R_l$, 18,600,000; free-stream Mach number $M_0$, 1.99.
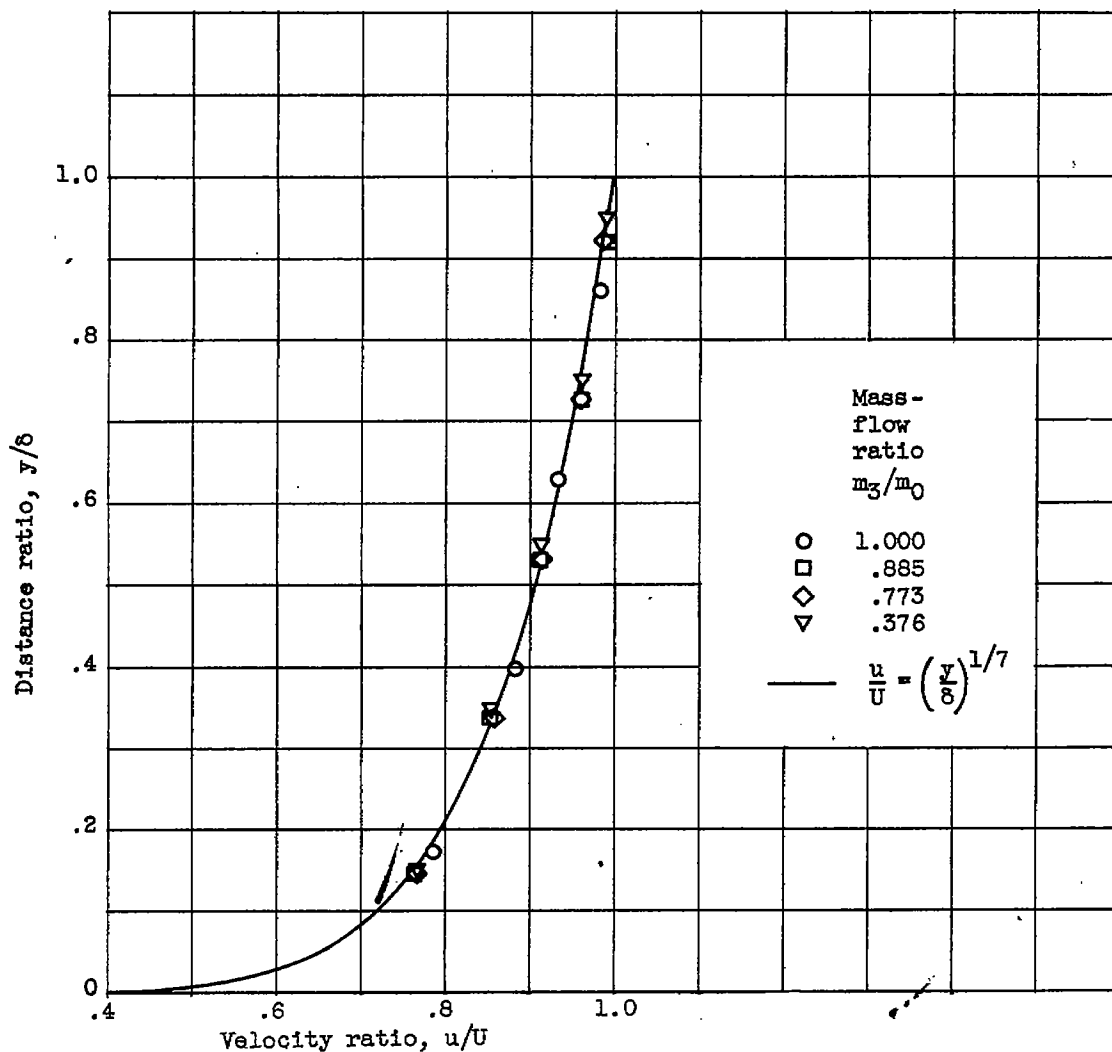
Figure 6. - Nondimensional boundary-layer profiles. Reynolds number $R_l$, 18,600,000; free-stream Mach number $M_0$, 1.99.
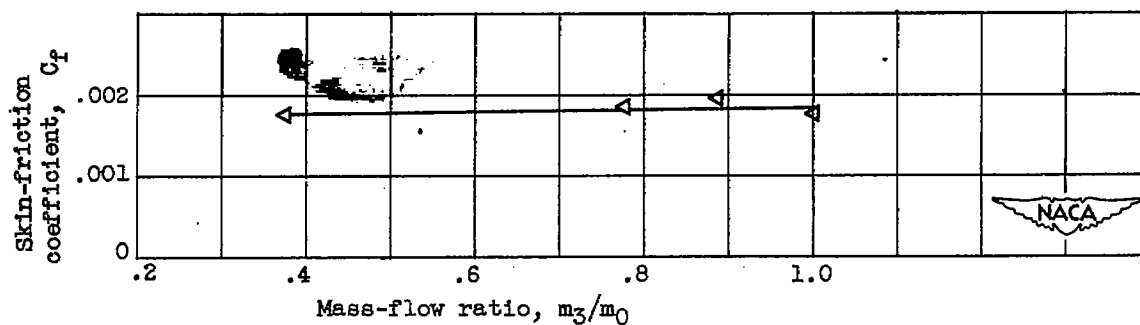


Figure 7. - Variation of skin-friction drag coefficient with mass-flow ratio. Reynolds number $R_l$, 18,600,000; free-stream Mach number $M_0$, 1.99.